UC Santa Cruz
UC Santa Cruz Previously Published Works

Title

Effects of core formation on the Hf–W isotopic composition of the Earth and dating of the Moon-forming impact

Permalink

https://escholarship.org/uc/item/0rb9k20r

Authors

Fischer, Rebecca A
Nimmo, Francis

Publication Date

2018-10-01

DOI

10.1016/j.epsl.2018.07.030

Peer reviewed

Effects of core formation on the Hf–W isotopic composition of the Earth and dating of the Moon-forming impact

Rebecca A. Fischer[1,2,3,*] and **Francis Nimmo**[2]

[1]Harvard University, Department of Earth and Planetary Sciences

[2]University of California Santa Cruz, Department of Earth and Planetary Science

[3]Smithsonian National Museum of Natural History, Department of Mineral Sciences

Abstract

Earth's core formation set the initial compositions of the core and mantle. Various aspects of core formation, such as the degree of metal–silicate equilibration, oxygen fugacity, and depth of equilibration, have significant consequences for the resulting compositions, yet are poorly constrained. The Hf–W isotopic system can provide unique constraints on these aspects relative to other geochemical or geophysical methods. Here we model the Hf–W isotopic evolution of the Earth, improving over previous studies by combining a large number of N-body simulations of planetary accretion with a core formation model that includes self-consistent evolution of oxygen fugacity and a partition coefficient of tungsten that evolves with changing pressure, temperature, composition, and oxygen fugacity. The effective average fraction of equilibrating metal is constrained to be $k > 0.2$ for a range of equilibrating silicate masses (for canonical accretion scenarios), and is likely <0.55 if the Moon formed later than 65 Ma. These values of k typically correspond to an effective equilibration depth of ~0.5–0.7× the evolving core–mantle boundary pressure as the planet grows. The average mass of equilibrating silicate was likely at least 3× the impactor's silicate mass. Equilibration temperature, initial fO_2 initial differentiation time, semimajor axis, and planetary mass (above ~0.9 $M_\oplus$) have no systematic effect on the ^{182}W anomaly, or on $f^{Hf/W}$ (except for fO_2), when applying the constraint that the model must reproduce Earth's mantle W abundance. There are strong tradeoffs between the effects of k, equilibrating silicate mass, depth of equilibration, and timing of core formation, so the terrestrial Hf–W isotopic system should be interpreted with caution when used as a chronometer of Earth's core formation. Because of these strong tradeoffs, the Earth's tungsten anomaly can be reproduced for Moon-forming impact timescales spanning at least 10–175 Ma. Early Moon formation ages require a higher degree of metal–silicate equilibration to produce Earth's ^{182}W anomaly.

*Corresponding author. rebeccafischer@g.harvard.edu. Phone: 617.384.6992.

1. Introduction

The segregation of Earth's metallic core from its silicate mantle was one of the most significant geochemical events in our planet's history. Understanding how and when this process occurred informs our knowledge of the accretion and earliest state of our planet, its modern-day core composition, the timing of Moon formation, and many other phenomena. The Hf–W system is one of the most widely used geochemical tools for dating Earth's core formation (e.g., Jacobsen, 2005; Kleine et al., 2002; Touboul et al., 2007; Yin et al., 2002). It can also be used to explore the nature of the core formation process by comparing measurements with numerical models (e.g., Halliday et al., 1996; Harper and Jacobsen, 1996; Kleine et al., 2004a; Nimmo and Agnor, 2006; Rudge et al., 2010).

^{182}Hf decays into ^{182}W with a half-life of 8.9 Ma (e.g., Kleine et al., 2009), the same order of magnitude as terrestrial planet accretion timescales. During core formation, moderately siderophile W is mostly sequestered into a planet's core. Halfnium is lithophile, so if ^{182}Hf is alive during core formation, it will remain in the mantle and decay into ^{182}W, creating an excess of mantle ^{182}W relative to other W isotopes. The Hf–W system is therefore sensitive to core formation timing (e.g., Halliday et al., 1996; Harper and Jacobsen, 1996; Jacobsen, 2005). Previous studies have shown that the Hf–W system is also sensitive to the siderophility of W (Halliday and Lee, 1999; Yu and Jacobsen, 2011) and the mechanism of core formation, such as the extent of metal equilibration (e.g., Dahl and Stevenson, 2010; Kleine et al., 2004a; Nimmo and Agnor, 2006; Nimmo et al., 2010; Rudge et al., 2010) and the extent of silicate equilibration (e.g., Deguen et al., 2014; Harper and Jacobsen, 1996; Morishima et al., 2013). Both Nimmo et al. (2010) and Rudge et al. (2010) found that Earth's ^{182}W anomaly is best reproduced when ~40% of the incoming metal equilibrates with the mantle, for example. A greater extent of metal–silicate equilibration reduces the tungsten anomaly significantly, requiring faster growth to reproduce Earth's ^{182}W anomaly (e.g., Rudge et al., 2010).

In most of these previous models, the partitioning behavior of W was treated as a constant and constrained to match the present-day mantle tungsten concentration, whereas experimental data show that it depends strongly on pressure (P), temperature (T), oxygen fugacity (fO_2), and composition (Cottrell et al., 2009; Ohtani et al., 1997; Righter and Drake, 1999; Righter et al., 1997; Shofner, 2011; Shofner et al., 2014; Siebert et al., 2011; Wade et al., 2012; and references therein), which changed within the Earth's interior as it grew. More sophisticated models of core formation now exist in which elements partition between metal and silicate in multiple stages as the Earth grows and oxygen fugacity evolves self-consistently (e.g., Fischer et al., 2017; Rubie et al., 2011), but these models have focused on elemental chemistry and have not included isotopic calculations.

The goal of this study is to combine Hf–W modeling with a core formation model (Fischer et al., 2017) to better understand the process of core formation. Relative to previous Hf–W models, we introduce several novel concepts. Here the partitioning behavior of W varies with P, T, fO_2, and composition. A large number of accretion simulations are used for growth histories (Fischer and Ciesla, 2014), to illustrate how stochastic variability in accretion history affects the Hf–W system. Because we incorporate a full core formation

model, the composition of Earth's mantle provides additional constraints that the model must reproduce. This type of model can be used to improve interpretations of Hf–W measurements and to better understand the timing and mechanism of core formation.

2. Numerical methods

Modeling Hf–W isotopic evolution requires an understanding of impact history, modeling of core formation, and an isotopic model. Information about impact history was taken from a suite of 100 *N*-body simulations (Fischer and Ciesla, 2014), which provide plausible accretion histories of the planets (e.g., timing of impacts, masses/provenance of impactors). Fifty of the simulations are consistent with the Nice model (Circular Jupiter and Saturn, CJS), and fifty have Jupiter and Saturn on their modern-day orbits (Eccentric Jupiter and Saturn, EJS). CJS and EJS represent two of many possible models of Solar System formation, considered here as examples of growth histories for the Earth; other styles of accretion may have different implications (Section 6). The simulations began with ~80 Moon- to Mars-mass planetary embryos and ~3000 smaller planetesimals. When two bodies passed within the sum of their radii, they were assumed to merge (Section 6). After 200 Ma of orbital evolution, the 100 simulations had formed 73 Earth analogues, defined here as the largest surviving planet with a semimajor axis of 0.75–1.25 AU and a mass within a factor of 1.5 of Earth's mass ($M_\oplus$). These Earth analogues have a mean mass of $1.0 \pm 0.2\ M_\oplus$ and semimajor axis of 0.98 ± 0.14 AU.

In the post-processing of these simulations, they are combined with a core formation model (Fischer et al., 2017, which uses similar methodology to Rubie et al., 2011). Each body is assigned an initial composition, then the model steps through the accretion histories of all bodies, allowing them to undergo high *P-T* metal–silicate equilibration with each impact. Compositions of the resulting cores and mantles are calculated for a variety of major, minor, and trace elements, with the metal–silicate partitioning behaviors of these elements calculated as functions of P, T, fO_2, and composition as constrained by experimental data (e.g., Fischer et al., 2015). Pressures are determined using Earth's density variations with depth as a pseudo equation of state (Fischer et al., 2017). Oxygen fugacity is expressed in log units relative to the iron–wüstite (IW) oxygen fugacity buffer and is approximated as:

$$\Delta \text{IW} \approx 2\log\left(\frac{X_{\text{FeO}}}{X_{\text{Fe}}}\right) \quad (1)$$

where X_{FeO} is the FeO content of the mantle and X_{Fe} is the Fe content of the core, expressed as mole fractions. An initial oxygen fugacity is prescribed, but subsequently it is evolved self-consistently (e.g., Rubie et al., 2011) according to experimentally-determined partitioning data, to ensure that only viable fO_2 histories are produced.

Metal–silicate partitioning of W has been added to the core formation model of Fischer et al. (2017), based on the experimental results of Shofner (2011) and Shofner et al. (2014). This work combines new W metal–silicate partitioning data obtained in a laser-heated diamond anvil cell at pressures up to 50 GPa with data from many previous studies (Cottrell et al.,

2009; Ohtani et al., 1997; Righter and Drake, 1999; Righter et al., 1997; Siebert et al., 2011; Wade et al., 2012; and references therein). The partition coefficient D of tungsten is expressed as a function of fO_2, P, T, silicate melt composition (SiO_2, Al_2O_3, CaO, and MgO), and metallic melt composition (C and S, which are not utilized here; see Section 6). For tungsten, $D_w = X_w/X_{wO_3}$, while Hf is assumed to be perfectly lithophile.

Between impacts, radiogenic ^{182}W is produced in the mantle from the decay of ^{182}Hf, and with each impact, the ^{182}W abundance is modified by a core formation event. Earth's mantle W isotopic composition is tracked as a ^{182}W anomaly, defined using epsilon notation:

$$\varepsilon_{182W} = \left[\frac{(X^{182W}/X^{183W})}{(X^{182W}/X^{183W})_{CHUR}} - 1 \right] \times 10^4 \quad (2)$$

equal to 1.9 ± 0.1 for the present-day Earth (Kleine et al., 2002, 2004b; Yin et al., 2002), where X^{182W} and X^{183W} are the ^{182}W and ^{183}W contents of the mantle, respectively, expressed as mole fractions; and *CHUR* indicates the composition of a chondritic uniform reservoir. Earth's mantle Hf/W ratio is described as:

$$f^{Hf/W} = \frac{(X^{180Hf}/X^{183W})}{(X^{180Hf}/X^{183W})_{CHUR}} - 1 \quad (3)$$

equal to 13.6 ± 4.3 for the present-day Earth (Kleine et al., 2009). However, there is disagreement over this value; for example, Dauphas et al. (2014) report an Earth $f^{Hf/W} = 25.4 \pm 4.2$ based on a reevaluation of literature data, with the main difference from the Kleine et al. (2009) value being in the chondritic Hf/Th ratio assumed. Here we apply the constraint that Earth's mantle W abundance must be reproduced on average (Palme and O'Neill, 2007; though there is significant uncertainty in this value, see Section 6), which typically corresponds to $f^{Hf/W} \approx 13.6$, depending on the core mass fraction. Other values used in the isotopic calculations, such as $^{182}W/^{184}W_{initial}$, $^{182}Hf/^{180}Hf_{initial}$, and $^{180}Hf/^{183}W_{CHUR}$, are taken from Kleine et al. (2009).

Adjustable parameters within the model include the effective depth (pressure and temperature) of metal–silicate equilibration, fraction k of incoming metal that equilibrates, mass of equilibrating silicate, thermal profile, initial fO_2, and timing of first differentiation event. The depth of equilibration, expressed as a fixed fraction of the core–mantle boundary (CMB) pressure, was allowed to vary between 0 and 1. The depth for each set of model parameters was chosen such that the Earth's mantle W abundance (Palme and O'Neill, 2007) was always reproduced on average, ensuring that each set of model parameters was consistent with observations while allowing constraints to be placed on the other variables investigated. Exactly matching Earth's mantle W abundance often resulted in a slight mismatch to other compositional parameters (Section 6) but was necessary to ensure correct modeling of the Hf–W system. The fraction of equilibrating metal k was also varied between 0 and 1, and the mass of equilibrating silicate was varied between that of the impactor's

silicate only and the entire impactor+target silicate (the "whole mantle" case), with the composition of the silicate varied accordingly. In most model runs, the temperature was pinned to the mantle liquidus (Andrault et al., 2011), though in one case it was varied from −500 to +1500 K to assess temperature effects. Initial fO_2 was usually fixed at IW−3.5 (3.5 log units below IW; equivalent here to $D_{Fe} = 56$), while values from IW−4.5 to IW−2 were tested, usually with a spatially uniform distribution. In most model runs, all bodies differentiated at the start of the N-body simulations, though differentiation upon first impact was also tested. Stochastic variability was introduced by the N-body simulations, which include, for example, a last giant impact time ranging from ~10 Ma to ~175 Ma.

3. Evolution of the [182]W anomaly

One of the advances made here is the W partition coefficient D_w varying as a function of P, T, fO_2, and composition, rather than being held fixed as in most previous studies (e.g., Nimmo et al., 2010; Rudge et al., 2010) or undergoing a single step-wise change (Halliday and Lee, 1999). Yu and Jacobsen (2011) were the first to have D_w evolve with P and T, but with an imposed or fitted oxygen fugacity evolution and an analytical growth curve. This improvement is significant because D_w varies by ~3 orders of magnitude over the conditions of Earth's core formation, causing behavior that has not been captured in most previous studies.

Figure 1 shows the evolution of planetary mass, mantle WO_3 abundance, and mantle [182]W anomaly in three representative Earth analogues, which have different growth histories but approximately the same final mass. In the first ~20 Ma, these planets accrete 0.25–0.6 $M_{\oplus}$. This corresponds to only ~0.5–5 ppb mantle WO_3 (equivalent to ~0.4–4 ppb mantle elemental W), due to W being more siderophile at low pressures. Because nearly all non-radiogenic W is partitioned into the core, a large fraction of mantle tungsten is [182]W, resulting in very large tungsten anomalies (up to ~300) at these early times. Over the next few tens of Ma, the [182]W anomalies reach maxima of 10–40. By 80 Ma, the planets have reached ~0.9 $M_{\oplus}$, most of their mantle tungsten has been accumulated, and their anomalies are down to 4–8. By the end of the simulations, these example Earth analogues have masses of nearly 1 $M_{\oplus}$ and 21–23 ppb mantle WO_3, compared to Earth's value of 20 ± 6 ppb WO_3 (or 16 ppb W) (Palme and O'Neill, 2007; note that the equilibration depth was chosen to match this value on average, Section 2). Final W anomalies are 0.5–3.4 epsilon units. This modeling approach, the first to include self-consistent variations in W partitioning based on evolving conditions inside the Earth, reveals real behavior in [182]W anomaly evolution not seen in previous studies (e.g., Dwyer et al., 2015; Nimmo and Agnor, 2006). Despite the large spikes in anomalies at early times, the final anomalies are similar to those of the Earth and previous studies (e.g., Nimmo et al., 2010).

4. Effects of core formation on Earth's [182]W anomaly

A number of previous studies (e.g., Kleine et al., 2004a; Nimmo et al., 2010; Rudge et al., 2010) demonstrated that k affects the [182]W anomaly, and several (e.g., Deguen et al., 2014; Harper and Jacobsen, 1996; Morishima et al., 2013) also considered variable extents of silicate equilibration. Here we revisit these effects incorporating variable W metal–silicate

partitioning, and also assess the effects of planetary mass, provenance, temperature, fO_2, and timing of initial differentiation. All model results discussed in this section are presented in Tables S1 and S2.

4.1. Effects of the fraction of incoming metal equilibrating, *k*

It is likely that not all accreted metal equilibrated with the growing Earth's mantle, for example in cases of large, differentiated impactors (e.g., Deguen et al., 2011). In reality, the fraction of metal that equilibrated, *k*, probably depended on sizes and velocities of impactors and other factors (Section 6), though here we consider one constant effective value of *k* varied between 0 (core merging) and 1 (complete emulsification).

The fraction of equilibrating metal cannot be varied in isolation, because doing so affects other aspects of planetary chemistry (for example, the mantle's W abundance) (Fischer et al., 2017); here a compensating change in equilibration depth (*P-T*) is used as *k* is varied to maintain an Earth-like mantle composition. For a fixed mass of equilibrating silicate, a lower *k* requires greater depths to match the Earth's observed mantle W abundance (Figure 2), providing constraints on the effective depth of metal–silicate equilibration. Thus the median $f^{Hf/W}$ is constant as *k* is varied, due to the corresponding change in depth, which differs from previous studies (e.g., Nimmo et al., 2010).

The ^{182}W anomaly is larger with less equilibrating metal, in agreement with previous studies (e.g., Kleine et al., 2009; Nimmo et al., 2010), with a stronger effect seen at the lowest *k* (Figure 2). The error bars in Figure 2 reflect spread in the data due to stochastic variability from *N*-body simulations, in particular variations in final planetary mass (Section 4.3), *P-T* history, and timing of large impacts (Section 5). For lower *k*, more variability from impactor tungsten anomalies is preserved, resulting in more spread in the data (a similar effect occurs for $f^{Hf/W}$; Table S1). For whole mantle equilibration, Earth's ^{182}W anomaly is best matched with *k* = 0.4, with a range of *k* = 0.25–0.7 providing a match within a 68% two-sided probability region (Figure 2). These values are in excellent agreement with those found in previous studies (Nimmo et al., 2010; Rudge et al., 2010), though it is not obvious *a priori* that this should necessarily be the case, as one might expect the evolving W partitioning behavior to yield a different answer.

4.2. Effects of the mass of equilibrating silicate

There are several lines of evidence that Earth's entire mantle did not equilibrate with each impactor and/or did not fully melt upon impact, including experiments on turbulent entrainment (Deguen et al., 2014) and calculations of impact-induced melting (e.g., Nakajima and Stevenson, 2015). Reducing the equilibrating silicate mass increases the final ^{182}W anomaly (Figures 2 and S1). A match to the Earth's anomaly is achieved with whole mantle equilibration and *k* = 0.4 (Figure 2), or equilibrating with 5× the impactor's silicate mass and *k* = 0.55 (Figure S1), or with 3× the impactor's silicate and *k* = 1 (Figure 2), or some intermediate combination. Three times the impactor's silicate mass is the lowest mass of equilibrating silicate that produces a median ^{182}W anomaly matching that of the Earth. In reality, the equilibration efficiency of tungsten likely evolves as the Earth accretes (Supplemental Text; Figure S2). There is increased spread in the data at lower equilibrating

silicate masses (Figures 2 and S1), similar to the increased spread in the data at lower k (Section 4.1): a greater extent of equilibration (larger equilibrating silicate mass or higher k) erases much of the variability in ^{182}W anomaly seen in the Earth's impactors.

4.3. Effects of planetary mass and accretion history

Not all Earth analogues produced in the N-body simulations have a mass of exactly 1 $M_\oplus$. Variations in planetary mass contribute slightly to our stated 68% two-sided confidence intervals for ^{182}W anomalies (e.g., Figure 2) and significantly to those for $f^{Hf/W}$ (Table S1); actual confidence intervals for a 1 $M_\oplus$ planet would be smaller. This variability in planetary mass can be used to evaluate the effects of planetary mass on ^{182}W anomalies more generally. There is a moderate correlation between these parameters (Figure 3, upper panel) (correlation coefficient of −0.58, where −1 indicates a perfect negative correlation and 0 indicates no correlation), with the scatter in the data indicating that planets of any mass considered here may develop an Earth-like ^{182}W anomaly. However, the maximum anomaly increases approximately exponentially with decreasing planetary mass (Figure 3, upper panel), because tungsten's strongly siderophile behavior in smaller bodies evolves to more moderate behavior at higher pressures. For the same reason, there is a strong, non-linear dependence of mantle $f^{Hf/W}$ on planetary mass, with larger planets having a lower $f^{Hf/W}$ (lower mantle Hf/W ratio) (Figure 3, lower panel). These mass effects vary with the degree of equilibration, since less equilibration results in retention of a lower pressure signature from the accreted bodies regardless of final planetary mass. The higher maximum ^{182}W anomaly for smaller bodies (Figure 3, upper panel) is a consequence of the higher $f^{Hf/W}$ of these objects, as well as the more siderophile behavior of W at lower pressures; the scatter in the tungsten anomalies arises from the stochastic nature of impact events. This result (Figure 3) suggests that fragments ejected from planets with a Mars-like mass (or smaller) and similar oxidation state to the Earth could be identified by their high ^{182}W anomalies and $f^{Hf/W}$. Note that Mars, while smaller than the Earth, is significantly more oxidized as measured by its mantle X_{FeO}, resulting in its low $f^{Hf/W}$ (Dauphas and Pourmand, 2011).

There is no correlation of the ^{182}W anomaly or $f^{Hf/W}$ with any aspect of planetary dynamics, such as the Earth analogue's final semimajor axis or its mass-weighted semimajor axis, a measure of provenance (e.g., Fischer et al., 2018). Even if a gradient in initial fO_2 is imposed, there is no correlation, because this change in initial oxygen fugacity must be compensated by a change in equilibration conditions in order to reproduce the Earth's mantle composition (Section 4.4).

4.4. Effects of temperature, initial fO_2, and timing of initial differentiation

The effects of temperature, initial fO_2, and timing of initial differentiation of embryos/planetesimals on Earth's ^{182}W anomaly were also investigated. No one of these parameters can be changed while holding all other model parameters fixed; this would result in non-Earth-like mantle concentrations of tungsten and other elements. Therefore, as each parameter was adjusted, the equilibration depth was also varied to match the mantle's tungsten abundance (e.g., Section 4.1), ensuring a plausible set of model outcomes. Effects of these variables on one Earth analogue (final mass of 0.94 $M_\oplus$) were tested to explore sensitivity to them.

The temperature of equilibration relative to the liquidus (Andrault et al., 2011) was varied from −500 K to +1500 K, which required varying the equilibration depth from 0.64 to 0.30 times the CMB pressure to ensure that Earth's mantle W abundance was always reproduced. The resulting changes are small: the ^{182}W anomaly increased by 0.07 epsilon units and $f^{Hf/W}$ decreased by 0.44 (Figure 4, left panel). Increasing the equilibration temperature does have differential effects on other aspects of mantle chemistry, for example by decreasing mantle NiO and increasing mantle FeO and CoO and core Si and O for a constant mantle WO_3 (Table S2), because these elements have different *P-T* dependences of their metal–silicate partitioning behaviors (Fischer et al., 2017).

The oxygen fugacity (Eq. 1) at which initial equilibration occurred was varied between IW–4.5 and IW–2, requiring a variation in equilibration depth from 0.62 to 0.25 times the CMB pressure. Starting with initial oxygen fugacities of IW–4.5 to IW–2 and evolving fO_2 self-consistently as a planet grows (e.g., Rubie et al., 2011) results in final oxidation states of IW–2.9 to IW–2.0 and final core mass fractions of 0.44 to 0.24, compared to the Earth's value of 0.32. These variations have virtually no effect on the ^{182}W anomaly, which decreases by 0.04 with increasing fO_2 over this range when including corresponding changes in depth to match the mantle W abundance (Figure 4, center panel). $f^{Hf/W}$ decreases by 7.4, despite the constant mantle W content, because the lower core mass fraction dilutes mantle Hf. Like temperature, changes in fO_2 can change other aspects of mantle chemistry relative to W (Fischer et al., 2017).

The effects of initially differentiating each body at the start of the *N*-body simulations or upon first impact were also evaluated (e.g., Nimmo and Agnor, 2006). These effects are modulated by reequilibration upon impact; the two cases are identical in the limit of $k = 1$. Changing the differentiation time from the start of the simulations to the first impact of each body decreases the ^{182}W anomaly by 0.1 for $k = 0.6$, or by 0.5 for $k = 0.2$ (Figure 4, right panel). There is no effect on $f^{Hf/W}$.

5. The timing of the Moon-forming impact

Many previous studies have dated the Moon-forming giant impact to later than ~50 Ma using a variety of methods (e.g., 62^{+90}_{-10} Ma, Touboul et al., 2007; 70–160 Ma in a two-stage model, Rudge et al., 2010), while some studies have found earlier formation ages (e.g., 30 Ma, Jacobsen, 2005). The Earth analogues in the *N*-body simulations used here accrete their last embryos at ~10–175 Ma, though those with earlier accretion have a larger late veneer mass (Fischer and Ciesla, 2014; Jacobson et al., 2014); this tradeoff may offer some bounds on the timing of the last giant impact (Jacobson et al., 2014), considering the geochemical limits on the mass of the late veneer (e.g., Dauphas and Marty, 2002).

Simulations with later Moon-forming impacts generally require lower k for the same equilibrating mantle mass to match the Earth's observed ^{182}W anomaly (Figures 5a, S3). For whole mantle equilibration, Moon-forming impacts at ~50 Ma match Earth's tungsten anomaly for $k = 0.4$–0.55, while Moon-forming impacts at >150 Ma imply $k = 0.25$–0.4 (Figure 5a). For equilibration with 3× the impactor's silicate mass, higher fractions of metal equilibrating are required ($k = 0.55$–0.85 for Moon-forming impacts at ~50 Ma and 0.4–0.55

for >150 Ma; Figure S3). Similarly, simulations with later Moon-forming impacts generally require less equilibrating mantle mass for the same k (Figure 5b). In the case of $k = 0.55$, Moon-forming impacts at ~50 Ma typically require equilibration with >4× the impactor's silicate mass (up to whole mantle equilibration), while impacts at >150 Ma imply equilibration with 2–4× the impactor silicate mass (Figure 5b). For the right combination of model parameters, nearly all Earth analogues produced in the N-body simulations can match Earth's [182]W anomaly regardless of the timing of the Moon-forming impact, suggesting that the terrestrial Hf–W system may not be providing tight constraints on the timing of the Moon-forming impact and cessation of Earth's core formation. In fact, the Moon itself may provide a stronger constraint on its formation time, with most lunar isotopic data consistent with relatively late formation: the most reliable Sm–Nd, Pb–Pb, and Lu–Hf ages of a wide range of lunar rocks are 200–230 Ma (Borg et al., 2015, and references therein), and there are a lack of resolvable [182]W anomaly variations across lunar materials (Kruijer and Kleine, 2017).

The Hf/W ratio ($f^{\mathrm{Hf/W}}$) varies with the timing of the Moon-forming impact, but correlates most strongly with planetary mass (Section 4.3; Figure S4). Almost all Earth mass planets are consistent with Earth's $f^{\mathrm{Hf/W}}$ within uncertainty regardless of the Moon-forming impact timescale or the extent of metal–silicate equilibration, in part because the equilibration depth was chosen to match Earth's mantle W content.

The effects of k, equilibrating silicate mass, and the timing of the Moon-forming impact are significantly entangled with one another. In the future, timing of Moon formation may be better understood by using independent constraints on k and equilibrating mantle mass, for example from impact modeling and analogue experiments (e.g., Deguen et al., 2011, 2014). Alternatively, improved independent constraints on the age of the Moon, for example from isotopic dating, would offer insight into the style of Earth's core formation.

Requiring Earth's late veneer mass to be <0.02 $M_\oplus$ (compared to a geochemical upper bound of ~0.005 $M_\oplus$; e.g., Dauphas and Marty, 2002) generally excludes Moon-forming impact dates of <65 Ma (Fischer and Ciesla, 2014; Jacobson et al., 2014). To reproduce the Earth's [182]W anomaly with Moon-forming impacts at >65 Ma, equilibrating with between 3× the impactor's silicate mass (Figure S3) and the whole mantle (Figure 5a) requires $k = 0.2$–0.55. This constraint on k appears to hold for a variety of model conditions and Moon formation ages. Since k is the upper bound on any element's equilibration efficiency as defined by Deguen et al. (2014), this efficiency must be   0.55 (see Supplementary Information).

6. Limitations, complications, and future work

It is important to consider the limitations of numerical modeling in addressing such complex issues as core formation. For example, this model treats metal–silicate equilibration as occurring at a constant fraction of the CMB pressure. Equilibration depth likely varied based on magma ocean depth, which in turn depends on impact timing, velocity, angle, mass, and spatial distribution, atmosphere, and other factors. The P-T signature that any parcel retains likely also depends on the degree of emulsification upon impact, sinking timescale, and time

spent at the magma ocean's base (e.g., Deguen et al., 2011, 2014: Rubie et al., 2003). Similarly, the amounts of equilibrating metal and silicate likely also varied between impacts (e.g., Deguen et al., 2011, 2014; Figure S2). There is a tradeoff between the amounts of metal and silicate equilibrating (Figure 2) (Deguen et al., 2014; Fischer et al., 2017), such that a large impact with core merging (low k) and extensive mantle melting (high equilibrating silicate mass) might exhibit similar equilibration efficiency as a smaller impact with higher k and lower equilibrating silicate mass, so this model may be broadly capturing the Earth's isotopic evolution accurately.

There is considerable uncertainty in the tungsten concentration in Earth's mantle. For example, while Palme and O'Neill (2007) report a mantle abundance of 20 ± 6 ppb WO_3 (equivalent to a mantle abundance of 16 ± 5 ppb elemental W), Arevalo and McDonough (2008) report 17 ± 13 ppb WO_3 (13 ± 10 ppb W), and McDonough and Sun (1995) report 37 $\pm$ a factor of two ppb WO_3 ($29 \pm$ a factor of two ppb W). Accordingly, there is also uncertainty in $f^{Hf/W}$, with estimates including 13.6 ± 4.3 (Kleine et al., 2009) and 25.4 ± 4.2 (Dauphas et al., 2014) (Section 2). Using a higher (lower) mantle tungsten abundance, corresponding to a lower (higher) $f^{Hf/W}$, would systematically decrease (increase) our calculated ^{182}W anomalies by an amount comparable to their uncertainties (typically up to ± 1 epsilon unit for the full range of reported $f^{Hf/W}$ and W concentrations). This level of added uncertainty approximately translates into ± 0.1 in k for the range of k applicable to Earth's core formation (Figure 2). As the mantle W concentration (or $f^{Hf/W}$) is refined in future studies, our constraints on k may therefore be changed by up to ± 0.1.

It is difficult to simultaneously perfectly reproduce the mantle abundances of W and other important trace elements, such as Ni and Co. In this work, the W abundance was used as the primary constraint to ensure accurate modeling of the Hf–W system, though other moderately siderophile elements (such as Ni and Co) can also provide valuable constraints on the Earth's evolution (e.g., Fischer et al., 2015, 2017; Jana and Walker, 1997; Ohtani et al., 1997; Righter and Drake, 1999; Righter et al., 1997; Rubie et al., 2011; Siebert et al., 2011). For most model conditions, matching the W abundance of Palme and O'Neill, 2007 typically results in mantle Ni, Co, and Fe contents that are lower than Earth's. This may be due to the large uncertainties and variability in reported tungsten abundances in Earth's mantle. Using a higher mantle tungsten abundance (lower $f^{Hf/W}$) than the 20 ppb WO_3 used here (Palme and O'Neill, 2007) would improve the fit between the W and Ni partitioning results. This discrepancy may also be partly caused by the scarcity of experimental data on W partitioning above ~25 GPa (Shofner, 2011; Shofner et al., 2014).

The difference in model conditions needed to match the mantle abundances of W and Ni is explored further in Supplemental Table S3. For a given degree of metal–silicate equilibration, the equilibration depth was varied to match either the mantle Ni or W abundance. In the case of whole mantle equilibration, this does not significantly affect the ^{182}W anomaly. In the case of equilibration with 3× the impactor's silicate mass (the minimum amount of silicate equilibration that can reproduce the Earth's ^{182}W anomaly on average, Section 4.2), increasing the depth of equilibration to match the mantle NiO abundance decreases the tungsten anomaly by ~10–20% depending on k. For both endmember values of equilibrating silicate mass, this depth increase also lowers $f^{Hf/W}$ by

~25%. These changes in both the ^{182}W anomaly and $f^{Hf/W}$ are well within the 68% two-sided confidence interval of the calculation. Matching the mantle Ni abundance results in mantle W abundances of 26–28 ppb, within the uncertainties of the measured values.

The discrepancy between W partitioning and that of other elements may be related to C and S, which were not included here because their abundances and partitioning behavior at high pressure are poorly understood. Based on available W partitioning data at lower *P-T,* carbon increases D_w (e.g., Cottrell et al., 2009; Jana and Walker, 1997; Righter and Drake, 1999; Shofner, 2011; Shofner et al., 2014; Siebert et al., 2011), while sulfur decreases D_w (Righter and Drake, 1999; Shofner, 2011; Shofner et al., 2014). Adding sulfur to the model would worsen the match with other trace elements, while adding carbon would improve the match.

The findings presented here are specifically applicable to EJS and CJS accretion scenarios, but these are only one possible type of growth history. For example, in the Grand Tack model, planets tend to form earlier (e.g., Walsh et al., 2011). This likely means that the Grand Tack model requires more extensive metal–silicate equilibration to reproduce Earth's ^{182}W anomaly (Figure 5) (Zube et al., 2017). Including fragmentation in the *N*-body simulations tends to form planets more slowly (e.g., Chambers, 2013), which should have the opposite effect (Figure 5) (Dwyer et al., 2015).

Future work may focus on other types of accretion scenarios, effects of the late veneer, or the isotopic composition of Mars. Geochemical studies indicate effects of late accretion to the Earth and Moon on the Hf–W system (e.g., Kruijer et al., 2015; Touboul et al., 2015); however, we cannot explore these effects due to the resolution of the *N*-body simulations used here. Previous studies have begun looking at the expected ^{182}W anomaly of Mars (e.g., Dauphas and Pourmand, 2011; Kleine et al., 2009; Nimmo and Agnor, 2006), but the methods used here cannot be rigorously applied to Mars in EJS/CJS simulations due to the small number of Mars analogues with the observed mass; this could be explored in future work using other types of simulations (e.g., Grand Tack) that have a higher probability of forming Mars. These methods could also be applied to test the probability of Earth and Theia having similar W anomalies, which could explain the Moon's Earth-like ^{182}W anomaly (e.g., Dauphas et al., 2014; Kruijer and Kleine, 2017).

7.   Conclusions

The model presented here represents a significant improvement over previous models of the Hf-W system in several ways. The W partition coefficient, D_w, varies with the evolution of pressure, temperature, oxygen fugacity, and composition in the Earth, and changes by ~3 orders of magnitude during Earth's accretion. In contrast, most previous studies held D_w fixed (e.g., Kleine et al., 2004a; Nimmo and Agnor, 2006; Nimmo et al., 2010; Rudge et al., 2010). This model includes many major and minor elements in the Earth, with self-consistent oxygen fugacity evolution, which allows model conditions to be chosen that satisfactorily reproduce the Earth's composition as well as its ^{182}W anomaly. No one parameter in the model may be varied in isolation, as done in previous studies, because doing so ensures a non-Earth-like mantle composition. Finally, we use 100 *N*-body simulations that form 73 Earth analogues. In contrast, previous studies used an idealized

growth curve for the Earth (e.g., Harper and Jacobsen, 1996; Rudge et al., 2010; Yu and Jacobsen, 2011) or 2–16 *N*-body simulations (Dwyer et al., 2015; Morishima et al., 2013; Nimmo and Agnor, 2006; Nimmo et al., 2010). Using a large number of realistic simulations is critical to see the variability among Earth analogues caused by stochastic variations in accretion history (e.g., Fischer and Ciesla, 2014).

Using these novel methods, the average fraction of equilibrating metal is broadly constrained to be $k = 0.2$–0.55 for any plausible equilibrating silicate mass, with this upper bound corresponding to a Moon formation age of 65 Ma or later as implied by Earth's late veneer mass. These values of k typically require effective equilibration depths of ~0.5–0.7× the core–mantle boundary pressure, which are tighter constraints than elemental chemistry provides (Fischer et al., 2017). The average equilibrating silicate mass was likely at least 3× the impactor's silicate mass. These constraints are all effective values, which are time-averaged over accretion; they provide a useful shorthand for discussing general conditions of core formation, but these conditions were likely not constant for every impact. Equilibration temperature, initial fO_2, initial differentiation time, semimajor axis, and planetary mass (above ~0.9 $M_\oplus$) have no systematic effect on the ^{182}W anomaly, or on $f^{Hf/W}$ (except for fO_2). Planetary mass can have an important effect on the ^{182}W anomaly in planets smaller than Earth.

The terrestrial Hf–W isotopic system is complex, with dependence on many interconnected parameters, so it should be interpreted with caution. There are strong tradeoffs between the effects of equilibrating metal fraction k, equilibrating silicate mass, equilibration depth, and timing of core formation. Due to these tradeoffs, we find matches to Earth's ^{182}W anomaly for Moon formation ages ranging from 10 Ma to 175 Ma, the full range investigated. Later ages require less equilibrating metal and/or silicate to reproduce Earth's tungsten anomaly.

Supplementary Material

Refer to Web version on PubMed Central for supplementary material.

Acknowledgments

References

Andrault D, Bolfan-Casanova N, Lo Nigro G, Bouhifd MA, Garbarino G, Mezouar M, 2011 Solidus and liquidus profiles of chondritic mantle: Implication for melting of the Earth across its history. Earth Planet. Sci. Lett. 304, 251–259. 10.1016/j.epsl.2011.02.006.

Arevalo R Jr., McDonough WF, 2008 Tungsten geochemistry and implications for understanding the Earth's interior. Earth Planet. Sci. Lett. 272, 656–665. 10.1016/j.epsl.2008.05.031.

Borg LE, Gaffney AM, Shearer CK, 2015 A review of lunar chronology revealing a preponderance of 4.34–4.37 Ga ages. Meteorit. Planet. Sci. 50, 715–732. 10.1111/maps.12373.

Chambers JE, 2013 Late-stage planetary accretion including hit-and-run collisions and fragmentation. Icarus 224, 43–56. 10.1016/j.icarus.2013.02.015.

Cottrell E, Walter MJ, Walker D, 2009 Metal–silicate partitioning of tungsten at high pressure and temperature: Implications for equilibrium core formation in Earth. Earth Planet. Sci. Lett. 281, 275–287. 10.1016/j.epsl.2009.02.024.

Dahl TW, Stevenson DJ, 2010 Turbulent mixing of metal and silicate during planet accretion – And interpretation of the Hf–W chronometer. Earth Planet. Sci. Lett. 295, 177–186. 10.1016/j.epsl. 2010.03.038.

Dauphas N, Marty B, 2002 Inference on the nature and the mass of Earth's late veneer from noble metals and gases. J. Geophys. Res. 107, 5129 10.1029/2001JE001617.

Dauphas N, Pourmand A, 2011 Hf–W–Th evidence for rapid growth of Mars and its status as a planetary embryo. Nature 473, 489–492. 10.1038/nature10077. [PubMed: 21614076]

Dauphas N, Burkhardt C, Warren PH, Teng F-Z, 2014 Geochemical arguments for an Earth-like Moon-forming impactor. Phil. Trans. R. Soc. A 372, 20130244 10.1098/rsta.2013.0244. [PubMed: 25114316]

Deguen R, Olson P, Cardin P, 2011 Experiments on turbulent metal–silicate mixing in a magma ocean. Earth Planet. Sci. Lett. 310, 303–313. 10.1016/j.epsl.2011.08.041.

Deguen R, Landeau M, Olson P, 2014 Turbulent metal–silicate mixing, fragmentation, and equilibration in magma oceans. Earth Planet. Sci. Lett. 391, 274–287. https://doi.Org/10.1016/j.epsl.2014.02.007.

Dwyer CA, Nimmo F, Chambers JE, 2015 Bulk chemical and Hf–W isotopic consequences of incomplete accretion during planet formation. Icarus 245, 145–152. 10.1016/j.icarus.2014.09.010.

Fischer RA, Ciesla FJ, 2014 Dynamics of the terrestrial planets from a large number of *N*-body simulations. Earth Planet. Sci. Lett. 392, 28–38. 10.1016/j.epsl.2014.02.011.

Fischer RA, Nakajima Y, Campbell AJ, Frost DJ, Harries D, Langenhorst F, Miyajima N, Pollok K, Rubie DC, 2015 High pressure metal–silicate partitioning of Ni, Co, V, Cr, Si, and O. Geochim. Cosmochim. Acta 167, 177–194. 10.1016/j.gca.2015.06.026.

Fischer RA, Campbell AJ, Ciesla FJ, 2017 Sensitivities of Earth's core and mantle compositions to accretion and differentiation processes. Earth Planet. Sci. Lett. 458, 252–262. 10.1016/j.epsl. 2016.10.025.

Fischer RA, Nimmo F, O'Brien DP, 2018 Radial mixing and Ru–Mo isoptope systematics under different accretion scenarios. Earth Planet. Sci. Lett. 482, 105–114. 10.1016/j.epsl.2017.10.055. [PubMed: 29622816]

Halliday AN, Lee D-C, 1999 Tungsten isotopes and the early development of the Earth and Moon. Geochim. Cosmochim. Acta 63, 4157–4179. 10.1016/S0016-7037(99)00315-4.

Halliday A, Rehkämper M, Lee D-C, Yi W, 1996 Early evolution of the Earth and Moon: New constraints from Hf–W isotope geochemistry. Earth Planet. Sci. Lett. 142, 75–89. 10.1016/0012-821X(96)00096-9.

Harper CL Jr., Jacobsen SB, 1996 Evidence for ^{182}Hf in the early Solar System and constraints on the timescale of terrestrial accretion and core formation. Geochim. Cosmochim. Acta 60, 1131–1153. 10.1016/0016-7037(96)00027-0.

Jacobsen SB, 2005 The Hf–W isotopic system and the origin of the Earth and Moon. Annu. Rev. Earth Planet. Sci. 33, 531–570. 10.1146/annurev.earth.33.092203.122614.

Jacobson SA, Morbidelli A, Raymond SN, O'Brien DP, Walsh KJ, Rubie DC, 2014 Highly siderophile elements in Earth's mantle as a clock for the Moon-forming impact. Nature 508, 84–87. 10.1038/nature13172. [PubMed: 24695310]

Jana D, Walker D, 1997 The impact of carbon on element distribution during core formation. Geochim. Cosmochim. Acta 61, 2759–2763. 10.1016/S0016-7037(97)00091-4.

Kleine T, Münker C, Mezger K, Palme H, 2002 Rapid accretion and early core formation on asteroids and the terrestrial planets from Hf–W chronometry. Nature 418, 952–955. 10.1038/nature00982. [PubMed: 12198541]

Kleine T, Mezger K, Palme H, Münker C, 2004a The W isotopic evolution of the bulk silicate Earth: Constraints on the timing and mechanisms of core formation and accretion. Earth Planet. Sci. Lett. 228, 109–123. 10.1016/j.epsl.2004.09.023.

Kleine T, Mezger K, Münker C, Palme H, and Bischoff A, 2004b ^{182}Hf–^{182}W isotope systematics of chondrites, eucrites, and martian meteorites: Chronology of core formation and early mantle

differentiation in Vesta and Mars. Geochim. Cosmochim. Acta 68, 2935–2946. 10.1016/j.gca. 2004.01.009.

Kleine T, Touboul M, Bourdon B, Nimmo F, Mezger K, Palme H, Jacobsen SB, Yin Q-Z, Halliday AN, 2009 Hf–W chronology of the accretion and early evolution of asteroids and terrestrial planets. Geochim. Cosmochim. Acta 73, 5150–5188. 10.1016/j.gca.2008.n.047.

Kruijer TS, Kleine T, Fischer-Gödde M, Sprung P, 2015 Lunar tungsten isotopic evidence for the late veneer. Nature 520, 534–537. 10.1038/nature14360. [PubMed: 25855296]

Kruijer TS, Kleine T, 2017 Tungsten isotopes and the origin of the Moon. Earth Planet. Sci. Lett. 475, 15–24. 10.1016/j.epsl.2017.07.021.

McDonough WF, Sun S. s., 1995 The composition of the Earth. Chem. Geol. 120, 223–253. 10.1016/0009-2541(94)00140-4.

Morishima R, Golabek GJ, Samuel H, 2013 N-body simulations of oligarchic growth of Mars: Implications for Hf–W chronology. Earth Planet. Sci. Lett. 366, 6–16. 10.1016/j.epsl.2013.01.036.

Nakajima M, Stevenson DJ, 2015 Melting and mixing states of the Earth's mantle after the Moon-forming impact. Earth Planet. Sci. Lett. 427, 286–295. 10.1016/j.epsl.2015.06.023.

Nimmo F, Agnor CB, 2006 Isotopic outcomes of N-body accretion simulations: Constraints on equilibration processes during large impacts from Hf/W observations. Earth Planet. Sci. Lett. 243, 26–43. https://doi.org/j.epsl.2005.12.009.

Nimmo F, O'Brien DP, Kleine T, 2010 Tungsten isotopic evolution during late-stage accretion: Constraints on Earth–Moon equilibration. Earth Planet. Sci. Lett. 292, 363–370. 10.1016/j.epsl. 2010.02.003.

Ohtani E, Yurimoto H, Seto S, 1997 Element partitioning between metallic liquid, silicate liquid, and lower-mantle minerals: Implications for core formation of the Earth. Phys. Earth Planet. Inter. 100, 97–114. 10.1016/S0031-9201(96)03234-7.

Palme H, O'Neill H.St.C., 2007 Cosmochemical estimates of mantle composition, in: Carlson RW (Ed.), Treatise on Geochemistry, Volume 2 Elsevier, pp.1–38. 10.1016/B0-08-043751-6/02177-0.

Righter K, Drake MJ, 1999 Effect of water on metal–silicate partitioning of siderophile elements: A high pressure and temperature terrestrial magma ocean and core formation. Earth Planet. Sci. Lett. 171, 383–399. 10.1016/S0012-821X(99)00156-9.

Righter K, Drake MJ, Yaxley G, 1997 Prediction of siderophile element metal–silicate partition coefficients to 20 GPa and 2800°C: The effects of pressure, temperature, oxygen fugacity, and silicate and metallic melt compositions. Phys. Earth Planet. Inter. 100, 115–134. 10.1016/S0031-9201(96)03235-9.

Rubie DC, Melosh HJ, Reid JE, Liebske C, Righter K, 2003 Mechanisms of metal–silicate equilibration in the terrestrial magma ocean. Earth Planet. Sci. Lett. 205, 239–255. 10.1016/S0012-821X(02)01044-0.

Rubie DC, Frost DJ, Mann U, Asahara Y, Nimmo F, Tsuno K, Kegler P, Holzheid A, Palme H, 2011 Heterogeneous accretion, composition and core–mantle differentiation of the Earth. Earth Planet. Sci. Lett. 301, 31–42. 10.1016/j.epsl.2010.22.030.

Rudge JF, Kleine T, Bourdon B, 2010 Broad bounds on Earth's accretion and core formatino constrained by geochemical models. Nat. Geosci. 3, 439–443. https://doi.org/NGEO872.

Shofner GA, 2011 High pressure redox geochemistry of tungsten in metal–silicate systems: Implications for core formation in the Earth Ph.D. dissertation, University of Maryland.

Shofner GA, Campbell AJ, Danielson L, Rahman Z, Righter K, 2014 Metal–silicate partitioning of tungsten from 10 to 50 GPa. Lunar Planet. Sci. XLV, 1267 (abstract).

Siebert J, Corgne A, Ryerson FJ, 2011 Systematics of metal–silicate partitioning for many siderophile elements applied to Earth's core formation. Geochim. Cosmochim. Acta 75, 1451–1489. 10.1016/j.gca.2010.12.013.

Touboul M, Kleine T, Bourdon B, Palme H, Wieler R, 2007 Late formation and prolonged differentiation of the Moon inferred from W isotopes in lunar metals. Nature 450, 1206–1209. 10.1038/nature06428. [PubMed: 18097403]

Touboul M, Puchtel IS, Walker RJ, 2015 Tungsten isotopic evidence for disproportional late accretion to the Earth and Moon. Nature 520, 530–533. 10.1038/nature14355. [PubMed: 25855299]

Wade J, Wood BJ, Tuff J, 2012 Metal–silicate partitioning of Mo and W at high pressures and temperatures: Evidence for late accretion of sulphur to the Earth. Geochim. Cosmochim. Acta 85, 58–74. 10.1016/j.gca.2012.01.010.

Walsh KJ, Morbidelli A, Raymond SN, O'Brien DP, Mandell AM, 2011 A low mass for Mars from Jupiter's early gas-driven migration. Nature 475, 206–209. 10.1038/nature10201. [PubMed: 21642961]

Yin Q, Jacobsen SB, Yamashita K, Blichert-Toft J, Télouk P, Albarède F, 2002 A short timescale for terrestrial planet formation from Hf–W chronometry of meteorites. Nature 418, 949–952. 10.1038/nature00995. [PubMed: 12198540]

Yu G, Jacobsen SB, 2011 Fast accretion of the Earth with a late Moon-forming giant impact. Proc. Natl. Acad. Sci. U.S.A. 108, 17604–17609. 10.1073/pnas.1108544108. [PubMed: 22006299]

Zube NG, Nimmo F, Jacobson SA, Fischer R, 2017 The trouble with building planets too quickly: Rapid accretion in Grand Tack simulations requires extremely efficient mantle equilibration of Hf–W. Lunar Planet. Sci. XL VIII, 1750 (abstract).
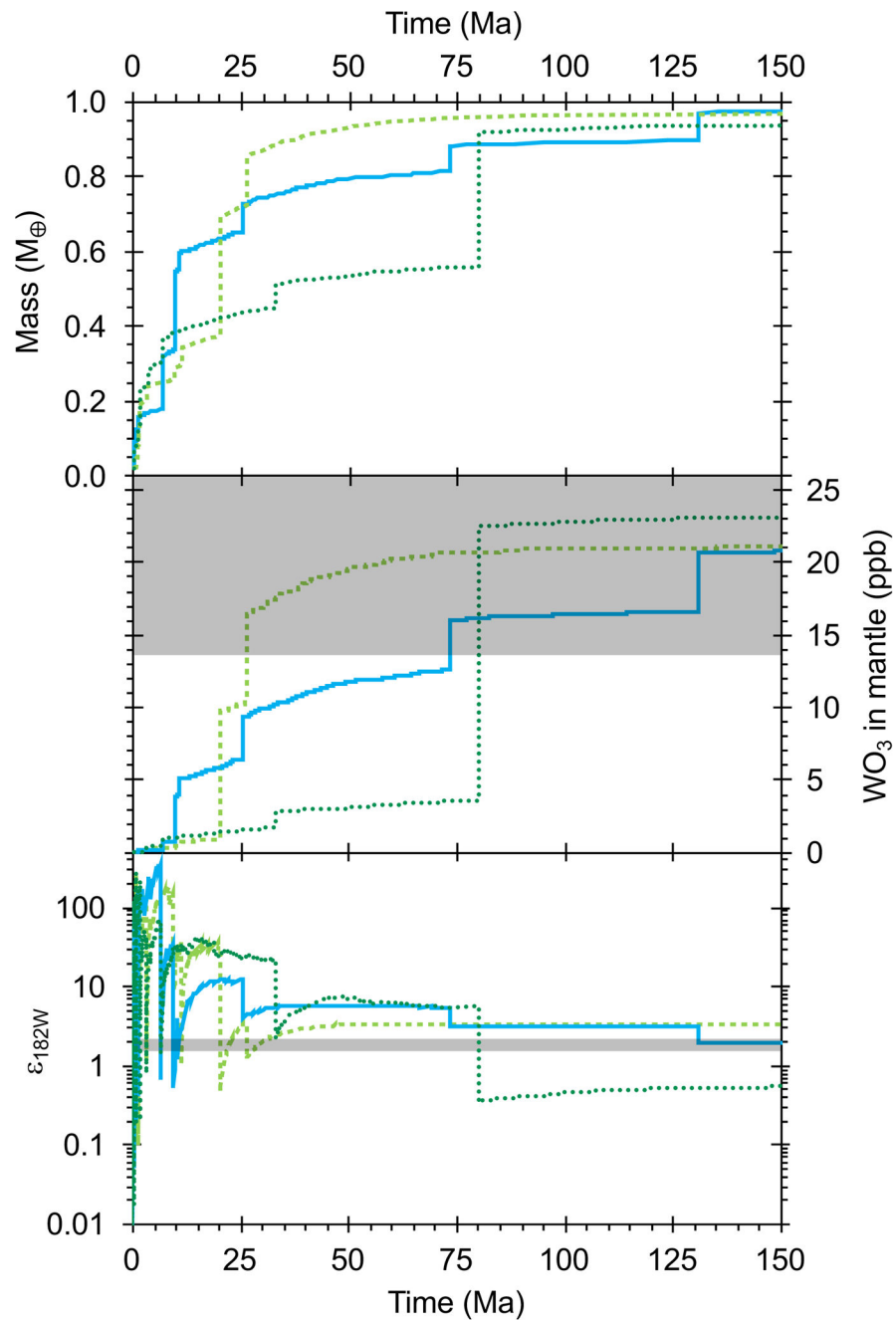
Figure 1:
The evolution of mass, mantle WO_3 content, and mantle ^{182}W anomaly for three example
Earth analogues (different colors/line types). Shaded regions indicate Earth values (Kleine et
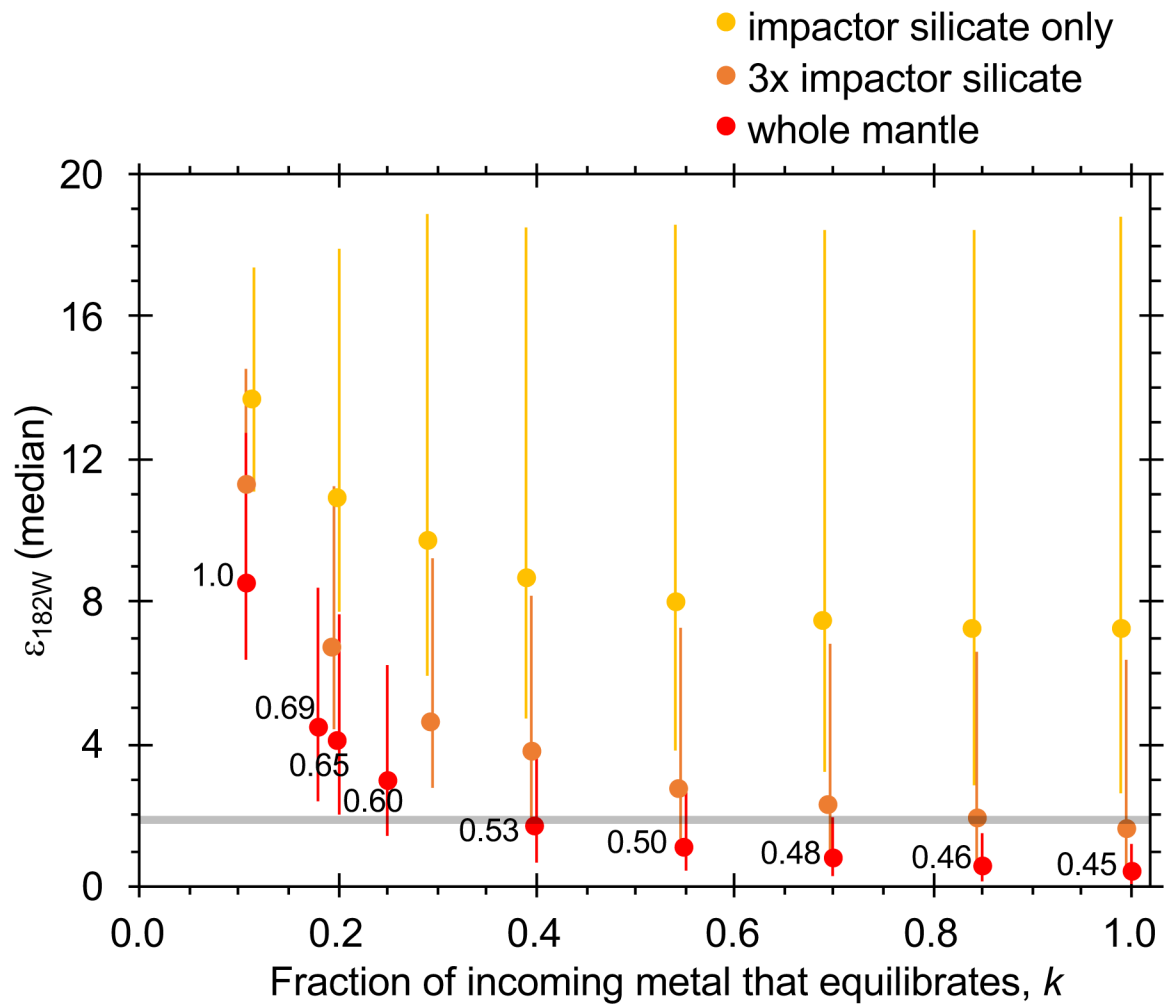al., 2004b; Palme and O'Neill, 2007).

Figure 2:
Effect of partial equilibration of metal and silicate on the resulting mantle ^{182}W anomaly.
Each data point is the median of 73 Earth analogues, with error bars representing a 68%
two-sided confidence interval. Shaded region indicates Earth value. Data labels are the depth
of equilibration (expressed as a fraction of the evolving core-mantle boundary pressure) for
the case of whole mantle equilibration. Data are slightly offset horizontally for clarity. Color
indicates amount of equilibrating silicate: impactor silicate only (yellow), impactor+target
silicate with a mass of 3× that of the impactor silicate (orange), and entire impactor+target
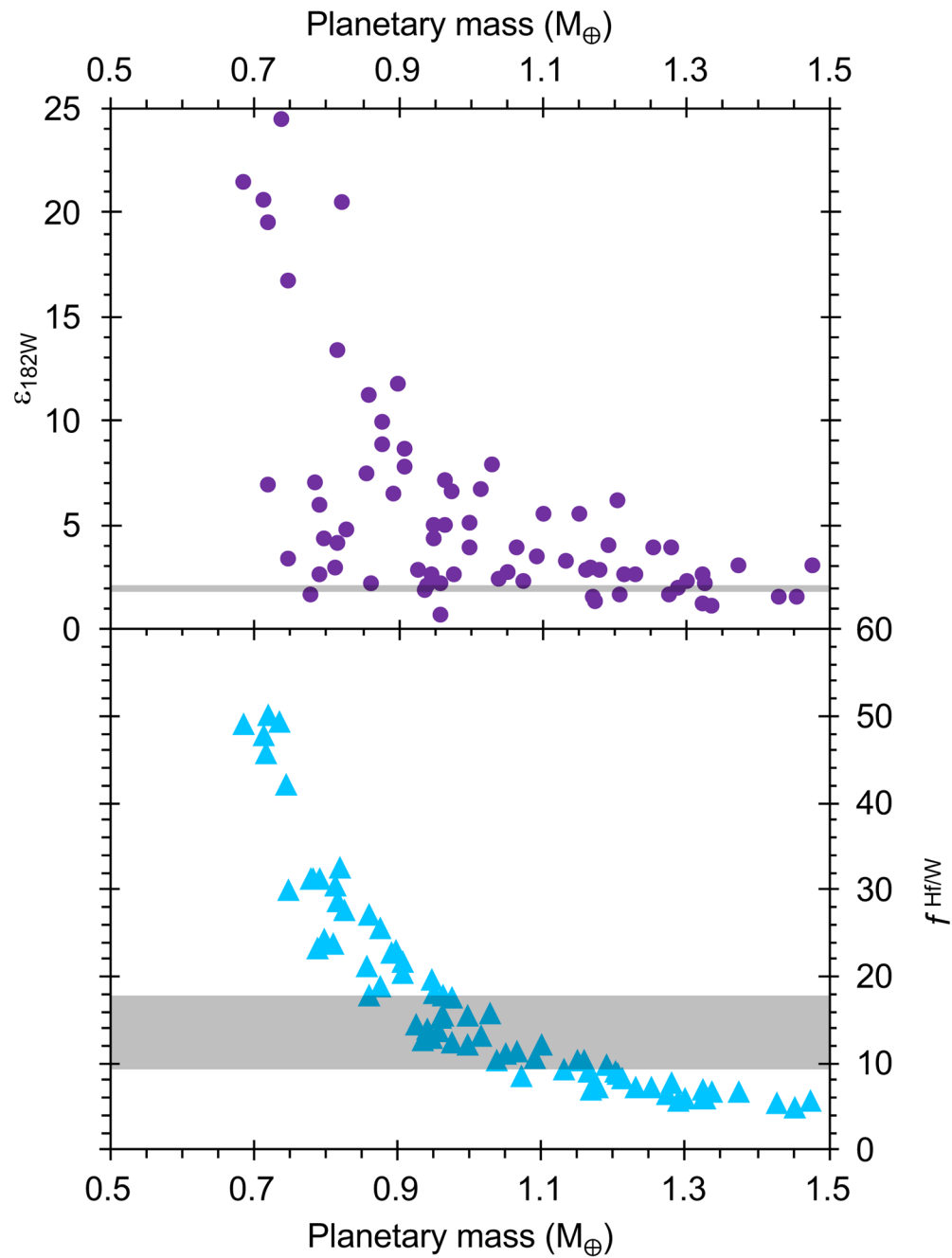silicate (red).

Figure 3:
Effect of planetary mass on the resulting mantle ^{182}W anomaly (upper panel) and $f^{Hf/W}$ (lower panel). Each data point represents one simulated Earth analogue. These results are for $k = 0.4$ and an equilibrating silicate mass of 3× that of the impactor's silicate. Shaded regions indicate Earth values (Kleine et al., 2004b, 2009).
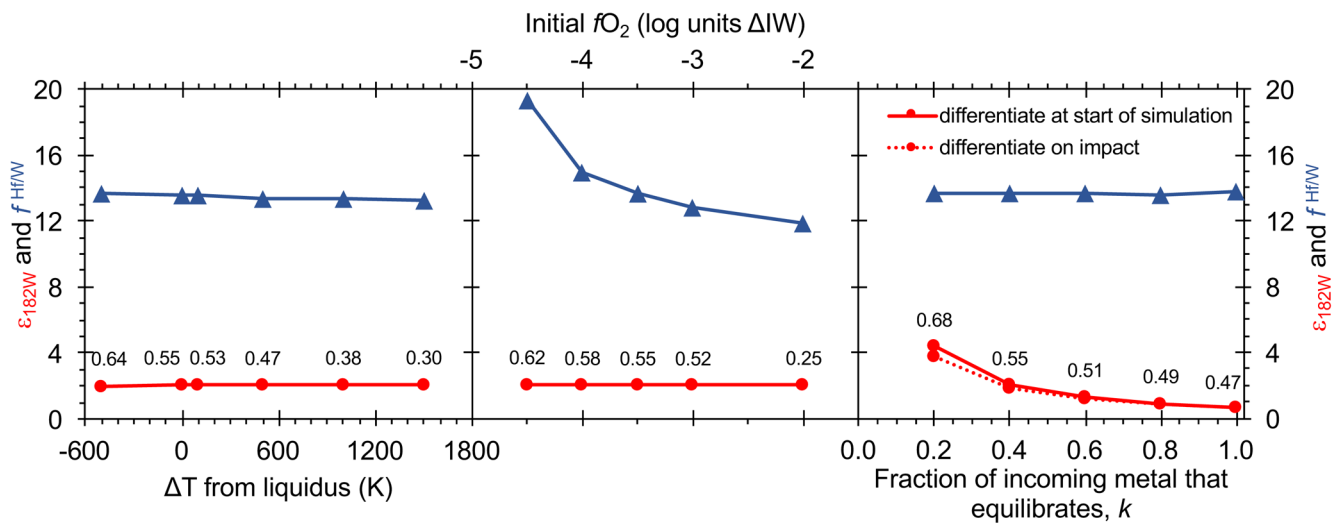
Figure 4:

Effects of temperature, oxygen fugacity, and timing of initial differentiation on the mantle
^{182}W anomaly (red circles and lines) and $f^{Hf/W}$ (blue triangles and lines) for one example
Earth analogue, with simultaneously varying equilibration depths chosen to match the
mantle W abundance. Left panel: Results of changing the equilibration temperature,
expressed as a deviation from the liquidus of Andrault et al. (2011). Center panel: Results of
changing the initial oxygen fugacity at which embryo and planetesimal compositions are
calculated at the start of the model. Right panel: Results of changing the time at which
embryos and planetesimals first differentiate with respect to the Hf–W system, either at the
onset of the *N*-body simulation (solid line) or when they experience their first impact (dotted
line) (e.g., Nimmo and Agnor, 2006), the effects of which are a function of the fraction of
incoming metal that equilibrates, *k*. Labels indicate the depth of equilibration, expressed as a
fraction of the core–mantle boundary pressure. Equilibration with three times the impactor's
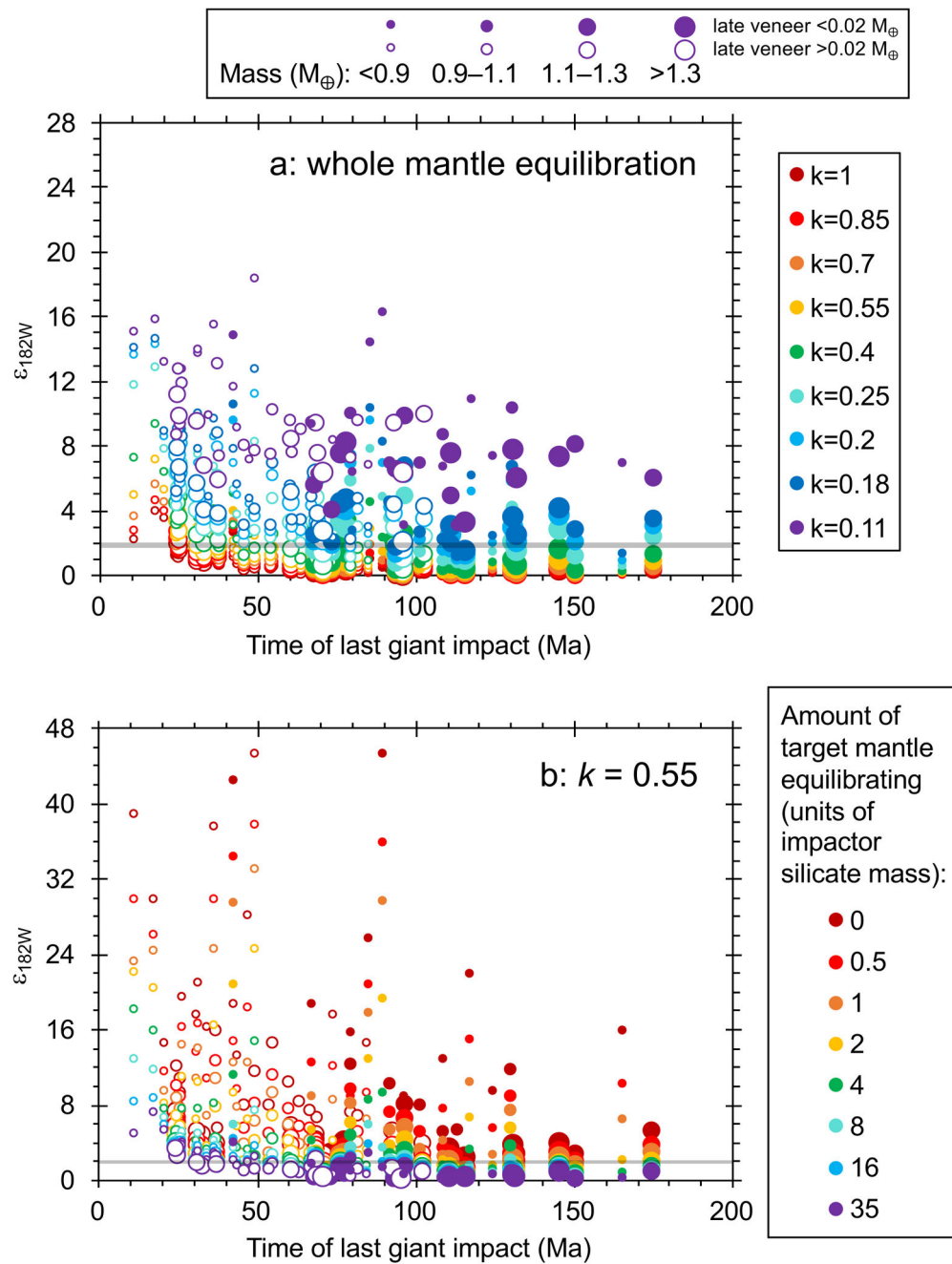silicate mass, $k = 0.4$, and initial oxygen fugacity of IW–3.5 were used except as noted.

Figure 5:

Effects of the timing of the Moon-forming impact, fraction of metal that equilibrates *k*, and equilibrating silicate mass on the resulting Earth [182]W anomaly. a) Effects of varying *k* for a fixed equilibrating silicate mass (whole mantle equilibration). b) Effects of varying the equilibrating silicate mass for a fixed fraction of equilibrating metal (*k* = 0.55). Entire impactor silicate is always equilibrated; amount of target silicate equilibrating is varied. Symbol size is proportional to planetary mass. Open (filled) symbols indicate Earth analogues whose late veneer mass is greater (less) than 0.02 M$_\oplus$. Each column of symbols

represents one simulation, with the different colored symbols within the column representing different model conditions. Shaded region is Earth value.